Catalysis Letters (2018) 148:2619–2626
https://doi.org/10.1007/s10562-018-2444-y

PERSPECTIVE

Highly Efficient Synthesis of C_2^+ Oxygenates from CO Hydrogenation Over Rh–Mn–Li/SiO_2 Catalyst: The Effect of TiO_2 Promoter

Dan Ding[1] · Jun Yu[1] · Qiangsheng Guo[1] · Xiaoming Guo[1] · Haifang Mao[1] · Dongsen Mao[1]

Received: 21 December 2017 / Accepted: 4 June 2018 / Published online: 11 June 2018

Abstract

The effect of titanium promotion on the catalytic performance of Rh–Mn–Li catalyst supported on PVP-modified SiO_2 for C_2^+ oxygenates synthesis from CO hydrogenation was investigated. The highest selectivity toward C_2^+ oxygenates (51.3%) was achieved over the RML/0.5Ti/SiO_2 catalyst. Characterization results indicates that the addition of Ti promotes the adsorption of geminal CO and the formation of Rh^+, which is favorable for the CO insertion into metal-CH_x band, and finally increases the selectivity of C_2^+ oxygenates.

Graphical Abstract

The effect of titanium promotion on the catalytic performance of Rh–Mn–Li catalyst supported on PVP-modified SiO_2 for C_2^+ oxygenates synthesis from CO hydrogenation was investigated. The highest selectivity toward C_2^+ oxygenates (51.3%) was achieved over the RML/0.5Ti/SiO_2 catalyst

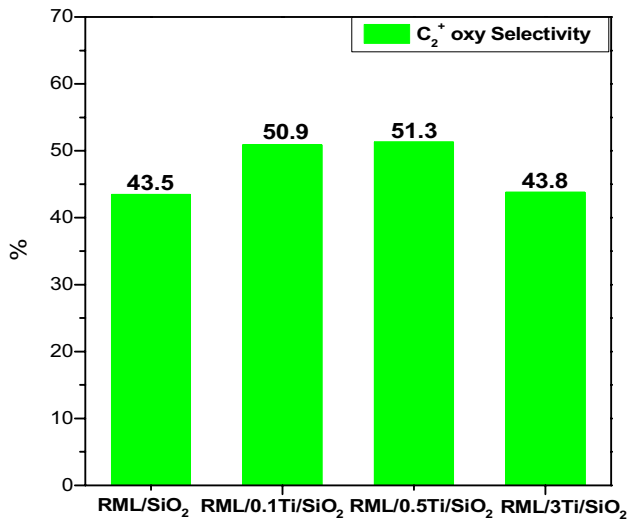

Keywords Rh–Mn–Li catalyst · CO hydrogenation · C_2^+ oxygenates · Titanium

1 Introduction

Nowadays, one of the largest social challenges is the demand for alternative sources of liquid fuels, which would reduce the greenhouse gas emission and depletion of fossil fuel resources [1]. A novel technology for the production of C_2 oxygenates, such as ethanol, acetaldehyde and acetic acid, from syngas

✉ Jun Yu
yujun@sit.edu.cn

✉ Dongsen Mao
dsmao@sit.edu.cn

[1] Research Institute of Applied Catalysis, School of Chemical and Environmental Engineering, Shanghai Institute of Technology, Shanghai 201418, China

derived from biomass, coal and natural gas, has attracted more and more attention [2–4]. Many catalysts for the synthesis of C_2 oxygenates have been reported in the literatures, such as Rh-based catalysts [5, 6], modified methanol synthesis catalysts [7, 8], modified Fischer–Tropsch catalysts [9] and Mo-based catalysts [10]. Among these, Rh-based catalysts have been thought as the best catalysts for the selective production of oxygenates via syngas conversion due to their excellent activity and selectivity in C_2 oxygenates [5, 11–14]. The influence of various supports on the catalytic activity of Rh-based catalysts has been widely reported [15]. SiO_2 has been the most frequently used support, because the Rh-based catalysts supported on it exhibit moderate activity and good selectivity toward C_2 oxygenates [16–18].

In addition to the effect of support, a wide range of promoters, including transition metals and rare-earth elements, also have significant influence on the selectivity of ethanol and other C_2^+ oxygenates [19–23]. It is well known that the addition of promoters, such as Mn and Li will greatly improve the catalytic performance of Rh-based catalysts. So far, the Rh–Mn–Li/SiO_2 catalyst is proven to be one of the most favorable catalyst systems for the synthesis of C_2^+ oxygenates from CO hydrogenation. Furthermore, some researchers studied the influence of iron promoter on catalytic properties of Rh–Mn–Li/SiO_2 for CO hydrogenation, and found that the addition of Fe can facilitate the transformation of dicarbonyl $Rh^+(CO)_2$ into H–Rh–CO, which is favorable for the formation of C_2^+ oxygenates [12, 22]. Wang et al. [24] studied the effect of ZrO_2 on the catalytic activity of Rh–Mn–Li/SiO_2. It was found that the addition of promoter Zr increased the amount of tilt-adsorbed CO species, which was suggested to be not only the precursor for CO dissociation but also the precursor for ethanol formation.

TiO_2, which employed in serving as the support in many literatures, could be favorable for the formation of C_2^+ oxygenates from CO hydrogenation [25–27]. However, it is rarely studied as a promoter. In our previous studies, it was found that the activity of the Rh–Mn–Li/SiO_2 catalyst for the synthesis of C_2^+ oxygenates from syngas was enhanced greatly when the commercial SiO_2 was replaced by the monodispersed SiO_2 that prepared by polyvinylpyrrolidone (PVP) modified Stöber method [28, 29]. Here, aiming to further improve the catalytic performance of this novel catalyst, various amounts of Ti were added into it and tested for the C_2^+ oxygenate synthesis from syngas. Moreover, insights into the effect of Ti on Rh–Mn–Li/SiO_2 for CO hydrogenation were demonstrated by a series of means.

2 Experimental

2.1 Catalyst Preparation

SiO_2 was prepared by a modified Stöber method [29]. Firstly, the solution A was prepared by mixing 21 ml tetraethylorthosilicate (TEOS) (99.5%, SCRC) with 50 ml anhydrous ethanol (99.7%, SCRC); the solution B was a mixture of 76 ml $NH_3{\cdot}H_2O$ (26 vol%, SCRC), 200 ml anhydrous ethanol and 1 g polyvinylpyrrolidone (PVP) (99.7%, SCRC). Secondly, the solution A was added slowly into the solution B in a flask under rapid stirring at 25 °C and reacted for 4 h. The white solid product was separated centrifugally at 7000 r.p.m for 5 min, washed with ethanol for three times and then dried at 90 °C for 12 h before being calcined in air at 600 °C for 4 h. Lastly, the SiO_2 prepared by the above method was impregnated with the aqueous solution of $Ti(OC_4H_9)_4$ (98%, SCRC), the paste dried at 90 °C for 12 h and finally obtained the support of xTi/SiO_2 (x = 0.1, 0.5, 3) after calcined in air at 600 °C for 4 h, where x represents the nominal weight percent of TiO_2 in the xTi/SiO_2 support after calcination.

A series of Rh-Mn-Li/xTi/SiO_2 catalysts were prepared by the incipient wetness impregnation method. $RhCl_3$ hydrate (Rh ~ 39 wt%, Fluka), $Mn(NO_3)_2{\cdot}6H_2O$ (99.99%, SCRC), $LiNO_3$ (99.95%, SCRC), and the supports mentioned above were used in catalyst preparation. Impregnated catalysts were dried at 90 °C for 4 h, and then at 110 °C overnight before calcined in air at 350 °C for 4 h. For all catalysts, Rh loading was 1.5 wt% and the weight ratio of Rh:Mn:Li = 1.5:1.5:0.07. Elemental analysis by inductively coupled plasma (ICP) revealed good agreement between the expected and experimental values. The obtained catalysts were denoted as RML/SiO_2, RML/0.1Ti/SiO_2, RML/0.5Ti/SiO_2, and RML/3Ti/SiO_2, respectively.

2.2 Catalyst Characterization

The metal loadings of the catalysts were determined by ICP-OES (PerkinElmerOptima 7000DV).

H_2 temperature-programmed reduction (TPR) of the catalysts were carried out in a quartz micro-reactor. 0.1 g of the sample was first pretreated at 350 °C in O_2/N_2 (molar ratio of $O_2/N_2 = 1/4$) for 1 h prior to a TPR measurement. During the TPR experiment, H_2/N_2 (molar ratio of $H_2/N_2 = 1/9$) mixture was used at 50 ml/min and the reduction temperature ramped from 50 to 500 °C (10 °C/min) while the effluent gas was analyzed with a thermal conductivity detector (TCD).

CO adsorption was studied using a Nicolet 6700 FTIR spectrometer equipped with a diffuse reflectance infrared

Fourier transform (DRIFT) cell with CaF_2 windows. The sample in the cell was pretreated in H_2/N_2 (molar ratio of $H_2/N_2 = 1/9$) at 400 °C for 2 h, followed by N_2 (50 ml/min) flushing at 400 °C for 0.5 h. During cooling down to the room temperature in N_2, a series of background spectra were taken at different temperatures. Then, 1% CO/N_2 (50 ml/min) was introduced into the cell and the IR spectra at the desired temperatures were recorded. After heating up to 300 °C in CO/N_2 mixture for 60 min, a H_2 flow (1 ml/min) was added into the flowing CO/N_2, and the IR spectra were recorded as a function of time. Ultrahigh-purity N_2, H_2 and CO used in the IR investigations was further purified by dehydration and deoxygenization. The spectral resolution was 4 cm^{-1} and the number of scans was 64.

The temperature-programmed surface reaction (TPSR) experiments were carried out as follows: after the catalyst was reduced at 400 °C in H_2/N_2 (molar ratio of $H_2/N_2 = 1/9$) for 2 h, it was cooled down to room temperature and CO was introduced for adsorption for 0.5 h; then, the H_2/N_2 mixture was swept again, and the temperature was increased at the rate of 10 °C/min with a quadrupole mass spectrometer (QMS, Balzers OmniStar 200) as the detector to monitor the signal of CH_4 (m/z = 15).

XPS measurements were performed using a Kratos Axis Ultra DLD spectrometer equipped with an Al Kα (1486.6 eV) X-ray source. The samples were pressed into small double side tap on a multi-specimen stage, then outgassed overnight under $p < 10^{-5}$ Pa in the preparation chamber and introduced into the analysis chamber where the pressure was around 10^{-4} Pa. The pass energy of the analyzer was set as 150 eV and the spot size was approximately 1.4 mm^2. For the XPS measurements of reduced catalysts, the as-prepared samples were reduced in situ at 400 °C for 1 h under the H_2 flow (10 ml/min) in the preparation chamber, and then the samples were transferred into the analysis chamber by a transfer rod under ultrahigh vacuum. The binding energies were calibrated relative to the C 1s peak from carbon contamination of the samples at 284.9 eV to correct for contact potential differences between the sample and the spectrometer.

2.3 Reaction

CO hydrogenation was performed in a fixed-bed micro-reactor with length ~ 350 mm and internal diameter ~ 5 mm. The catalyst (0.3 g) diluted with inert α-alumina (1.2 g) was loaded between quartz wool and axially centered in the reactor tube, with the temperature monitored by a thermocouple close to the catalyst bed. Prior to reaction, the catalyst was heated to 400 °C (heating rate ~ 3 °C/min) and reduced with H_2/N_2 (molar ratio of $H_2/N_2 = 1/9$, total flow rate = 50 ml/min) for 2 h at atmospheric pressure. The catalyst was then cooled down to the reaction temperature and the reaction started as gas flow was switched to a H_2/CO mixture (molar ratio of H_2/CO = 2, total flow rate = 50 ml/min) at 3 MPa. All post-reactor lines and valves were heated to 150 °C to prevent product condensation. The products were analyzed for both hydrocarbons and oxygenates on-line (FL GC 9720) using a HP-PLOT/Q column (30 m, 0.32 mm ID) with detection with a flame ionization detector (FID) and a TDX-01 column with a TCD. The conversion of CO was calculated based on the fraction of CO that formed carbon-containing products according to: $\%\text{Conversion} = (\sum n_i M_i / M_{CO}) \times 100\%$, where n_i is the number of carbon atoms in product i; M_i is the percentage of product i detected, and M_{CO} is the percentage of CO in the feed. The selectivity of a certain product was calculated based on carbon efficiency using the formula $n_i C_i / \sum n_i C_i$, where n_i and C_i are the carbon number and molar concentration of the ith product, respectively.

Table 1 CO hydrogenation reactivity data on different catalysts

Catalyst	Reaction temperature (°C)	CO Conv. (%)	Selectivity of products (C%)							STY(C_2^+ Oxy) g/(kg·h)
			CO_2	CH_4	MeOH	AcH	EtOH	C_2^+ HC[a]	C_2^+ Oxy[b]	
RML/SiO_2	300	24.8	3.6	14.1	2.7	21.5	14.7	36.1	43.5	290.4
RML/SiO_2	280	14.3	4.5	13.5	2.5	24.7	16.2	33.0	46.5	173.6
RML/0.1Ti/SiO_2	300	14.5	2.8	15.9	2.3	29.3	16.8	28.1	50.9	201.4
RML/0.5Ti/SiO_2	300	13.9	3.8	14.5	2.5	25.1	17.2	27.9	51.3	193.7
RML/3Ti/SiO_2	310	14.1	4.1	20.6	3.1	16.5	17.8	33.5	38.7	140.8
RML/3Ti/SiO_2	300	8.8	5.1	18.6	4.5	21.4	15.8	28.0	43.8	105.2

Reaction conditions: P = 3 MPa, Catalyst: 0.3 g, and flow rate = 50 ml/min (H_2/CO = 2), data taken after 15 h when steady state reached. experimental error: ± 5%

[a] C_2^+ HC denotes hydrocarbons containing two and more carbon atoms

[b] C_2^+ Oxy denotes oxygenates containing two and more carbon atoms

3 Results and Discussion

3.1 Catalytic Activities

The effect of Ti promoter on the catalytic properties of Rh–Mn–Li/SiO_2 catalyst in CO hydrogenation is shown in Table 1. Under the same reaction temperature (300 °C), the CO conversion of the RML/xTi/SiO_2 catalysts dropped with the increase of Ti loading. However, the selectivity of C_2^+ oxygenates increased notably over the catalysts supported on Ti modified SiO_2, indicating that the doping of Ti could accelerate the formation of C_2^+ oxygenates. In order to exclude the effect of conversion on selectivity, the catalysts of RML/SiO_2 and RML/3Ti/SiO_2 were also operated at 280 and 310 °C respectively, which achieved the similar CO conversions as RML/0.1Ti/SiO_2 and RML/0.5Ti/SiO_2 reacted at 300 °C. Under the similar CO conversion levels (~14%), the maximum of C_2^+ oxygenates selectivity was obtained at the RML/0.5Ti/SiO_2 catalyst. It is indicated that the selectivities of the catalysts are mainly controlled by the nature of the active center. On the other hand, the catalytic performance obtained at different reaction temperatures also indicated that the selectivity of hydrocarbon increased with the increase of CO conversion, while the selectivity of oxygenates decreased. Moreover, the yield of the C_2^+ oxygenates decreased sharply when the Ti content reached 3%.

3.2 H_2-TPR

Figure 1 shows the H_2-TPR profiles of various catalysts. It can be seen that all the catalysts exhibited three reduction peaks of H_2 consumption. According to the literatures [12, 30], the first two peaks were ascribed to the reduction of Rh_2O_3 not intimately contacting with Mn species (denoted as Rh(I) species) and of Rh_2O_3 intimately contacting with Mn species (denoted as Rh(II) species), respectively; and the third one was ascribed to the reduction of MnO_2. In addition, the peak at around 265 °C on RML/xTi/SiO_2 catalysts might be attributed to partial reduction of TiO_2 [31]. As shown in Fig. 1, with the increase of the loading of Ti, the reduction of Rh_2O_3 shifted to the lower temperature. According to Chen and co-workers [32], the smaller particles of Rh can be reduced at a lower temperature, thus the addition of Ti promoter can reduce the size of Rh particles and increase its dispersibility. Since the Rh(II) species only appears when there is a strong Rh–Mn interaction, the intensity of Rh(II) peak could determine the strength of Rh–Mn interaction. Based on the result of Table 2, the ratio of Rh(I)/Rh(II) decreased firstly and then increased with the increase of Ti loading, indicating that the appropriate content of Ti can enhance the interaction of Rh–Mn. It is conceivable that the intensity of this interaction may affect the reduction of Rh and change the state of the active site, and further influences the catalytic activity.

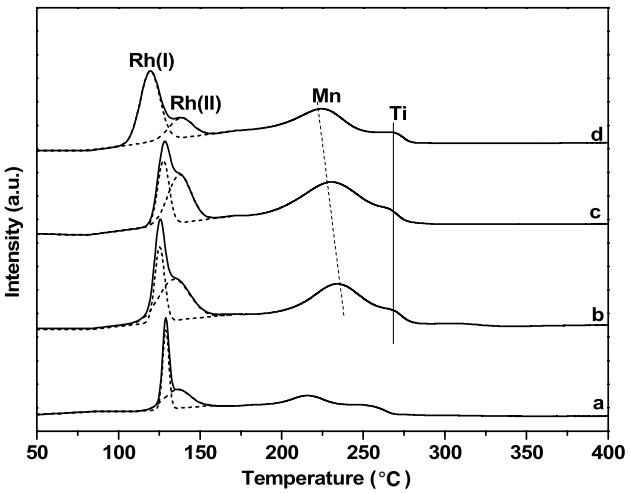

Fig. 1 TPR profiles of the catalysts: (*a*) RML/SiO_2, (*b*) RML/0.1Ti/SiO_2, (*c*) RML/0.5Ti/SiO_2, (*d*) RML/3Ti/SiO_2

3.3 FT-IR Study

Figure 2A shows the infrared spectra of adsorbed CO on the in situ reduced catalysts at 30 °C for 30 min. It can be seen that the IR spectrum was mainly composed by a doublet at ~2100 and ~2037 cm^{-1} and a band at around 2068 cm^{-1}. It is reported that the ~2068 cm^{-1} band can be ascribed to the linear adsorbed CO [CO(l)] and the doublet can be assigned to the symmetric and asymmetric carbonyl stretching of the gem-dicarbonyl $Rh^+(CO)_2$ [CO(gdc)] [33]. It is widely accepted that the CO(gdc) is formed on the Rh^+ sites and CO(l) is on the Rh^0 sites [17, 34]. Meanwhile, the bands centered at around 2173 and 2130 cm^{-1} can be attributed to gaseous CO [34]. It can be seen from Fig. 2A that the CO(l) could be observed on all the reduced catalysts and the intensity basically unchanged; However, the amount of CO(gdc) increased significantly after doping of Ti, which suggests that the number of Rh^+ increases. According to the literature [35], the Ti promoter can suppress the reduction of rhodium, so more Rh^+ ions would exist on the catalyst surface. It is well acknowledged that Rh^0 is the active center for CO dissociation, and Rh^+ sites are responsible for CO insertion to form intermediates of C_2^+ oxygenates [36, 37]. Thus, more Rh^+ sites existed on the catalyst surface imply more activity sites for CO insertion, which could improve the selectivity toward C_2^+ oxygenates.

Table 2 The ratios of reduction peaks of Rh_2O_3 for different forms

Catalyst	RML/SiO_2	RML/0.1Ti/SiO_2	RML/0.5Ti/SiO_2	RML/3Ti/SiO_2
Rh(I)/Rh(II)	1.60	0.55	0.66	3.01

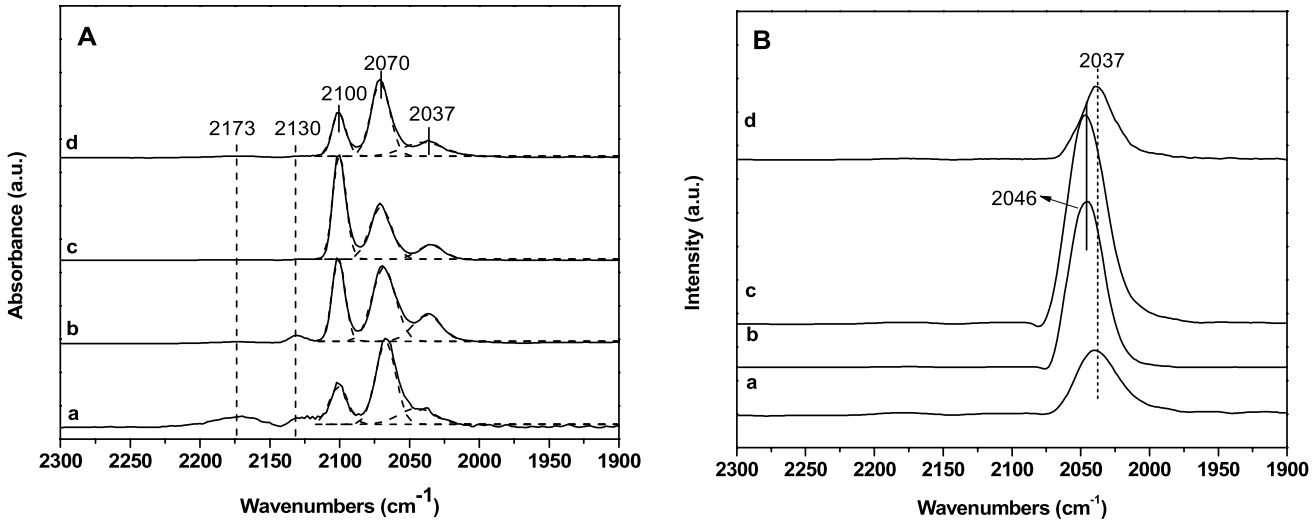

Fig. 2 The infrared spectra of absorbed CO in the CO/N_2 flow at 30 °C (**A**) and 300 °C (**B**): (*a*) RML/SiO_2, (*b*) $RML/0.1Ti/SiO_2$, (*c*) $RML/0.5Ti/SiO_2$, (*d*) $RML/3Ti/SiO_2$

Table 3 The ratios of peak areas of IR bands for the adsorbed CO species

Catalyst	RML/SiO_2	$RML/0.1Ti/SiO_2$	$RML/0.5Ti/SiO_2$	$RML/3Ti/SiO_2$
CO(gdc)/CO(l)[a]	0.31	0.99	1.95	0.50

[a]CO(gdc)/CO(l) denotes the peak area ratio of CO(gdc) versus CO(l) in Fig. 2A; experimental error: ±5%

On the other hand, it is worthy to note from Table 3 that the ratio of CO(gdc) versus CO(l) (Rh^+/Rh^0) on the catalysts increased in the order of $RML/SiO_2 < RML/3Ti/SiO_2 < RML/0.1Ti/SiO_2 < RML/0.5Ti/SiO_2$. Considering that H_2 is known to be adsorbed dissociatively on Rh^0 sites [38], it is inferred that a lower relative surface coverage of H* and CO* (θ_H/θ_{CO}) would be obtained on $RML/xTi/SiO_2$ catalyst due to their higher ratio of Rh^+/Rh^0 than that on RML/SiO_2. Gao et al. [39] observed that hydrogen-assisted CO dissociation is the rate-limiting step for CO hydrogenation, it is likely that the decrease of θ_H may restrain CO dissociation on the catalysts of $RML/xTi/SiO_2$, leading to the decrease of CO conversion.

Figure 2B shows the IR spectra of adsorbed species on the in situ reduced catalysts in CO/N_2 flow at 300 °C. It can be seen that, under the reaction temperature, the CO(gdc) of all the catalysts disappeared, only the CO(l) existed. It is indicated that the adsorption of CO were dominated by linear adsorption at the reaction temperature. Compared with the catalysts of RML/SiO_2 and $RML/3Ti/SiO_2$, the CO(l) band on the catalysts of $RML/0.1Ti/SiO_2$ and $RML/0.5Ti/SiO_2$ was shifted to higher frequency. The higher carbonyl stretching frequency of CO(l) may suggest less back-donation from Rh^0 into acceptor π^*_{CO} orbital, which infers that the Rh^0 sites are more electropositive caused by the electron-withdrawing effect of Ti. That is to say, the strength of the Rh–CO bond would be weakened by the appropriate amount of Ti doping. The weakened Rh–CO bond should be beneficial to the insertion of CO, resulting in the significant increase of C_2^+ oxygenates selectivity over the catalysts of $RML/0.1Ti/SiO_2$ and $RML/0.5Ti/SiO_2$.

Figure 3 shows the IR spectra taken after CO reaction with H_2 at 300 °C on the different catalysts. It can be seen that the IR spectra of adsorbed CO all existed in the form of CO (l) with different relative intensity after H_2 flushing as a function of time, which indicates that the CO (l) species is the mainly reactive species at the reaction temperature. The rates of decrease in the band for CO (l) on different catalysts followed the order as shown in Fig. 3: $RML/0.1Ti/SiO_2 < RML/0.5Ti/SiO_2 < RML/SiO_2 < RML/3Ti/SiO_2$. It is conceivable that, with the doping of Ti, the hydrogenation performance of the catalyst decreased sharply, thereby an appropriate content of Ti is conducive to the increase in the selectivity of C_2^+ oxygenates.

3.4 TPSR Study

Figure 4 shows the TPSR experiment over RML/SiO_2 catalysts with different Ti loadings. The profile of CH_4 formation indirectly indicates that the ability of CO dissociation related to the temperature of CH_4 formation, and that of hydrogenation correlated with the peak intensity of CH_4 formation. It can be seen from Fig. 4 that the peak of CH_4 formation of RML/SiO_2 catalyst was centered at around 245 °C, however, the CH_4 peak shifted to higher temperature on $RML/xTi/SiO_2$ catalysts, indicating that with the

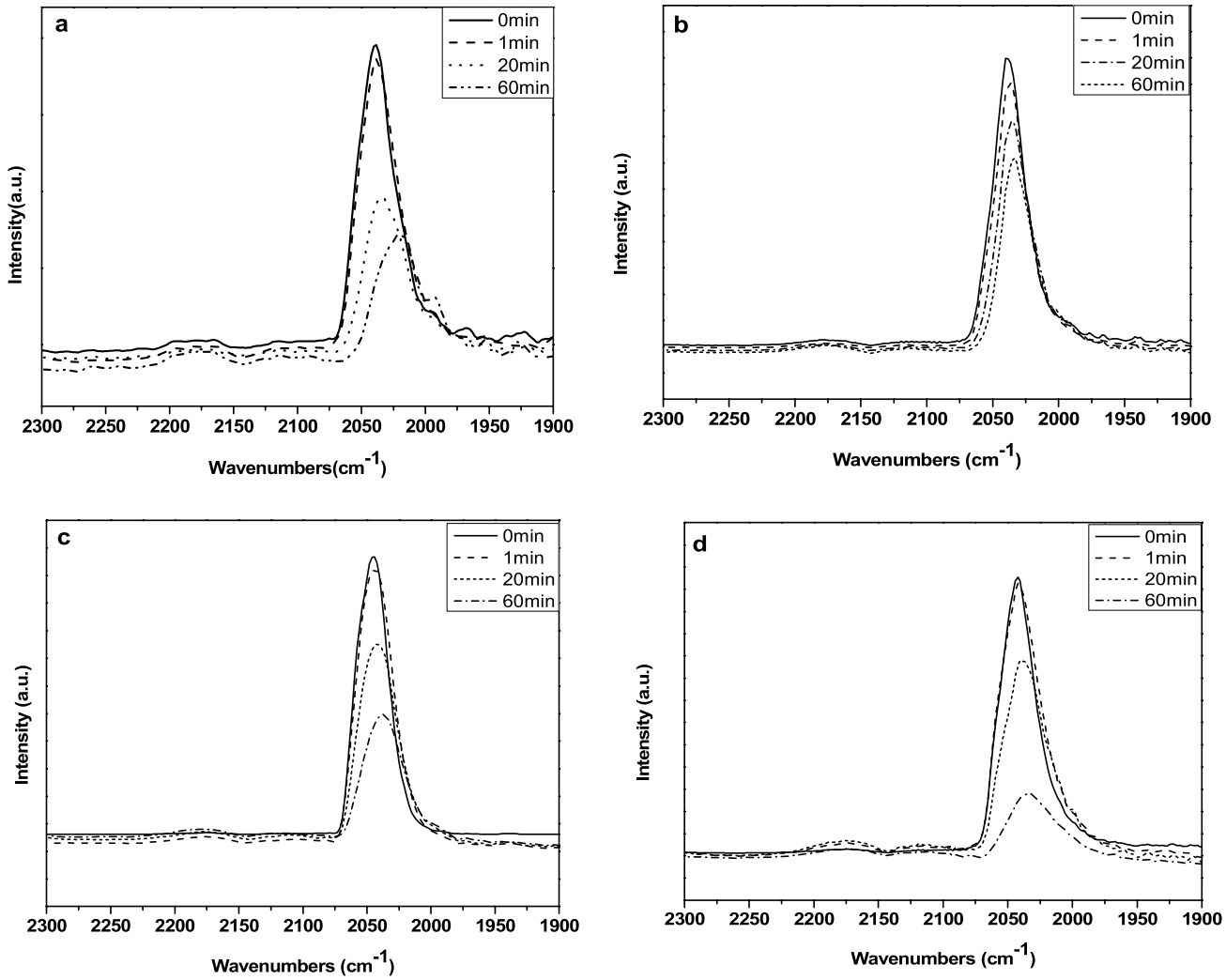

Fig. 3 The infrared spectra after CO hydrogenation on different catalysts at 300 °C: **a** RML/SiO_2, **b** RML/0.1Ti/SiO_2, **c** RML/0.5Ti/SiO_2, **d** RML/3Ti/SiO_2

introduction of Ti the dissociation ability of CO decreased, which is in line with the result of FT-IR. In addition, the area of CH_4 peak was different, following the order as shown in Table 4: RML/0.5Ti/SiO_2 < RML/SiO_2 < RML/0.1Ti/SiO_2 < RML/3Ti/SiO_2, in which the RML/0.5Ti/SiO_2 catalyst showed the weakest capability of hydrogenation. According to the literature [40], the formation of CH_4 from CH_x hydrogenation and the formation of C_2^+ oxygenates from CO insertion are the couple of competitive reaction. Therefore, the appropriate amount of Ti doping can promote the incorporation of CO into CH_X to form C_2^+ oxygenates precursors, resulting in an increase in the selectivity of C_2^+ oxygenates.

3.5 XPS Analysis

The Rh 3d core level spectra of different catalysts are displayed in Fig. 5. It can be found from Fig. 5A that two peaks observed at 309.8 and 314.6 eV could be attributed to Rh $3d_{5/2}$ and Rh $3d_{3/2}$ in all the fresh catalysts, suggesting that Rh species existed as Rh_2O_3. The Rh 3d core level spectrum of catalysts after in situ reduction are displayed in Fig. 5B. It is observed that the binding energy of the Rh $3d_{5/2}$ and Rh $3d_{3/2}$ peaks were located at 306.7 and 311.5 eV, indicating that Rh^0 is the major Rh species on all the reduced catalysts. However, it is obvious that the binding energy of Rh $3d_{5/2}$ and Rh $3d_{3/2}$ of RML/0.1Ti/SiO_2 and RML/0.5Ti/SiO_2 were shifted to higher values, suggesting that the electronic density on Rh particles decreased because of the electron-withdrawing property of Ti [37]. It is inferred that the Rh component in the catalysts of RML/0.1Ti/SiO_2 and RML/0.5Ti/SiO_2 existed in a nonstoichiometric state, which was between Rh^0 and Rh^+, that is to say, some partially positively charged $Rh^{\delta+}$ species also co-existed with Rh^0 on the surface of RML/0.1Ti/

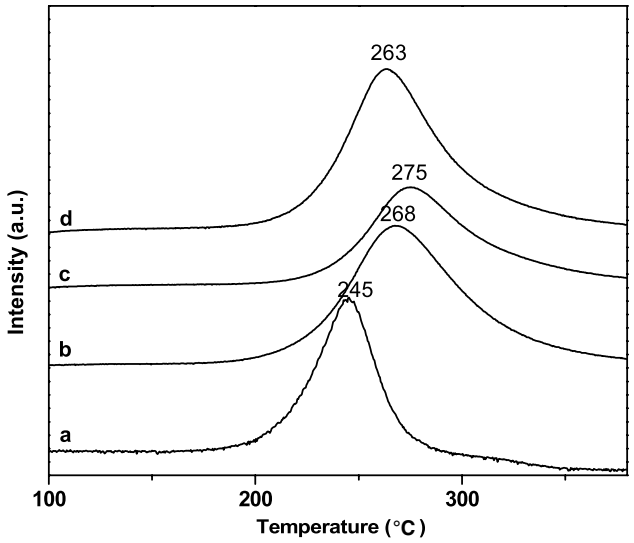

Fig. 4 The TPSR profiles of the different catalysts for CH_4 formation: (*a*) RML/SiO_2, (*b*) RML/0.1Ti/SiO_2, (*c*) RML/0.5Ti/SiO_2, (*d*) RML/3Ti/SiO_2

Table 4 The peak area of methane produced during TPSR in different catalyst

Sample	A_{CH4}
RML/SiO_2	1.0[a]
RML/0.1Ti/SiO_2	1.24
RML/0.5Ti/SiO_2	0.83
RML/3Ti/SiO_2	1.35

[a]The peak area of CH_4 formed in TPSR over the RML/SiO_2 catalyst was quantitative for one unit; experimental error: ±5%

SiO_2 and RML/0.5Ti/SiO_2 catalysts after reduction. Since Rh^+ ions are the active sites of CO insertion, the doping of Ti facilitates the progress of CO insertion, resulting in the increase in the selectivity of C_2^+ oxygenates, which is consistent with the result of FT-IR.

4 Conclusions

In this work, highly efficient Rh–Mn–Li/SiO_2 catalysts with and without doping of Ti were synthesized. The results show that the addition of Ti greatly affected the catalytic performance of Rh–Mn–Li/SiO_2 on CO hydrogenation: Ti could improve the activity for C_2^+ oxygenates formation, but decreased the CO conversion. Results from FT-IR and XPS indicates that the doping appropriate amount of Ti can stabilize Rh^+ ions, leading to more activity sites for CO insertion, finally resulting in the excellent catalytic performance of RML/0.1Ti/SiO_2 and RML/0.5Ti/SiO_2 for C_2^+ oxygenates synthesis. Combining the results of H_2-TPR and TPSR, it is proved that the appropriate amount of Ti loading can gradually strengthen the interaction between Rh and Mn. This interaction is conducive for a weakened hydrogenation ability, which is favorable for the CO insertion into metal-CH_X band, finally resulting in the excellent catalytic performance of RML/0.5Ti/SiO_2 for C_2^+ oxygenates synthesis.

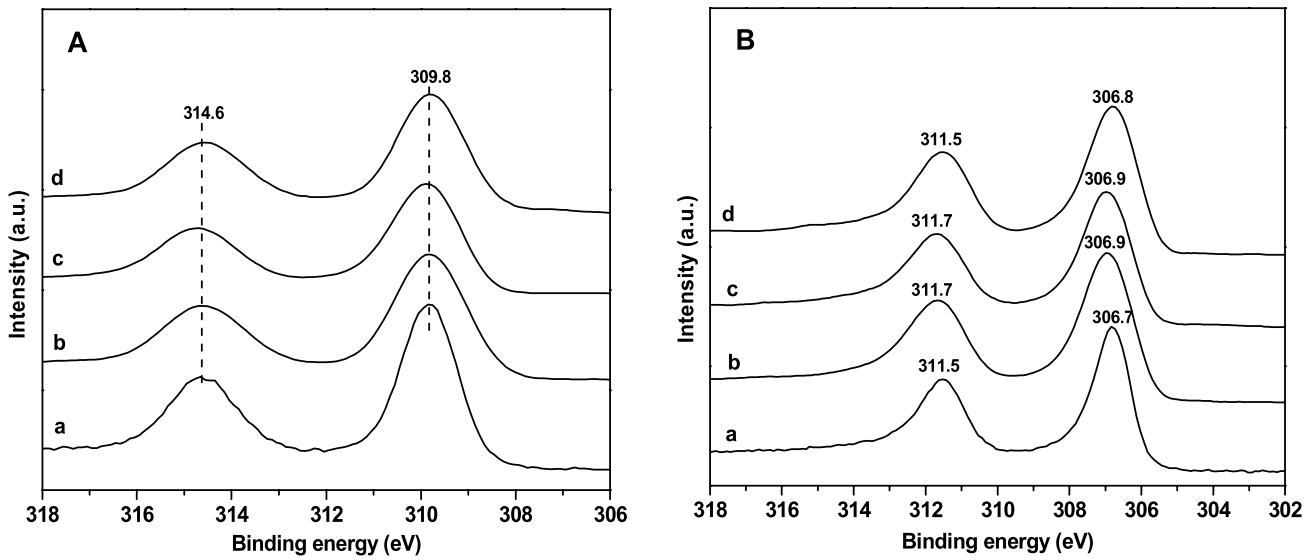

Fig. 5 Rh 3d XPS patterns of fresh (**A**) and reduced (**B**) catalysts: (*a*) RML/SiO_2, (*b*) RML/0.1Ti/SiO_2, (*c*) RML/0.5Ti/SiO_2, (*d*) RML/3Ti/SiO_2

Acknowledgements The authors gratefully acknowledge financial support from the Leading Academic Discipline Project of Shanghai Education Committee (J51503) and Shanghai Municipal Science and Technology Commission (13ZR1461900).

References

1. Rostrup-Nielsen JR (2005) Science 308:1421
2. Subramani V, Gangwal SK (2008) Energy Fuels 22:814
3. Mei DH, Rousseau R, Kathmann SM, Glezakou VA, Engelhard MH, Jiang W, Wang C, Gerber MA, White JF, Stevens DJ (2010) J Catal 271:342
4. Chen G, Guo CY, Zhang X, Huang Z, Yuan G (2011) Fuel Process Technol 92:461
5. Liu JJ, Guo ZY, Childers D, Schweitzer N, Marshall CL, Klie RF, Miller JT, Meyer RJ (2014) J Catal 313:158
6. Liu WG, Wang S, Wang SD (2016) Appl Catal A 510:227
7. Zuo ZJ, Wang L, Liu YJ, Huang W (2013) Catal Commun 34:69
8. Gupta M, Spivey JJ (2009) Catal Today 147:126
9. Fang YZ, Liu Y, Zhang LH (2011) Appl Cata A 397:183
10. Morrill MR, Thao NT, Agrawal PK, Jones CW, Davis RJ, Shou H, Barton DG, Ferrari D (2012) Catal Lett 142:875
11. Magee JW, Palomino RM, White MG (2016) Catal Lett 146:1771
12. Yin HM, Ding YJ, Luo HY, Zhu HZ, He DP, Xiong JM, Lin LW (2003) Appl Catal A 243:155
13. Gong JL, Yue HR, Zhao YJ, Zhao S, Zhao L, Lv J, Wang SP, Ma XB (2012) J Am Chem Soc 134:13922
14. Haider M, Gogate MR, Davis RJ (2009) J Catal 26:9
15. Fan ZL, Chen W, Pan XL, Bao XH (2009) Catal Today 147:86
16. Ho SW, Su YS (1997) J Catal 168:51
17. Jiang DH, Ding YJ, Pan ZD, Chen WM, Luo HY (2008) Catal Lett 121:241
18. Basu P, Panayotov D, Yates JT (1988) J Am Chem Soc 110:2074
19. Gao J, Mo XH, Chien ACY, Torres W, Goodwin JG (2009) J Catal 262:119
20. Li CM, Liu JM, Gao W, Zhao YF, Wei M (2013) Catal lett 143:1247
21. Haider MA, Gogate MR, Davis RJ (2009) J Catal 261:9
22. Yu J, Mao DS, Han LP, Guo QS, Lu GZ (2013) J Ind Eng Chem 19:806
23. Yu J, Mao DS, Ding D, Guo XM, Lu GZ (2016) J Mol Catal A: Chem 423:151
24. Wang Y, Luo HY, Liang DB, Bao XH (2000) J Catal 196:46
25. Egbebi A, Schwartz V, Overbury SH, Spive JJ (2010) Catal Today 149:91
26. Shen WJ, Okumura M, Matsumura Y, Masatake H (2001) Appl Catal A 213:225
27. Vannice MA (1982) J Catal 74:199
28. Yu J, Mao DS, Lu GZ, Guo QS, Han LP (2012) Catal Commun 24:25
29. Ding D, Yu J, Guo QS, Guo XM, Xiao XZ, Mao DS, Lu GZ (2017) RSC Adv 7:48420
30. Jiang DH, Ding YJ, Pan ZD, Li XM, Jiao GP, Li JW, Chen WM, Luo HY (2007) Appl Catal A 331:70
31. Han LP, Mao DS, Yu J, Guo QS, Lu GZ (2012) Catal Commun 23:20
32. Chen WM, Ding YJ, Luo HY, Yan L, Wang T, Pan ZD (2005) Chin J Appl Chem 22:470
33. Raskó J, Bontovics J (1999) Catal Lett 58:27
34. Solymosi F, Pasztor M (1986) J Phys Chem 90:5312
35. Chen WM, Ding YJ, Jiang DH, Pan ZD, Luo HY (2005) J Nat Gas Chem 14:199
36. Watson PR, Somorjai GA (1981) J Catal 72:347
37. Chuang SSC, Pien SI (1992) J Catal 135:618
38. Basu P, Panayotov D, Yates JT (1987) J Phys Chem 91:3133
39. Gao J, Mo XH, Goodwin JG (2009) J Catal 268:142
40. Choi YM, Liu P (2009) J Am Chem Soc 131:13054